Int. J. Heat Mass Transfer. Vol. 21, pp. 593–603

0017-9310/78/0501-0593 $02.00/0

MASS TRANSFER AT THE WALL AS A RESULT OF COHERENT STRUCTURES IN A TURBULENTLY FLOWING LIQUID

ROBERT S. BRODKEY, KENNETH N. MCKELVEY* and HARRY C. HERSHEY
Department of Chemical Engineering, The Ohio State University, Columbus, OH 43210, U.S.A.

and

STAVROS G. NYCHAS
Max-Planck-Institut für Strömungsforschung, D 34 Göttingen, F.R.G.

(*Received* 25 *July* 1975 *and in revised form* 1 *June* 1976)

Abstract—A direct numerical calculation of the instantaneous mass transfer at a solid boundary was made from a one-dimensional mass balance equation with the only input information being the normal velocity. This velocity was generated on the computer so as to have the gross characteristics of the normal velocity obtained from turbulence experiments. The average mass-transfer rate was adequately predicted. Other characteristics of the scalar field are reported.

NOMENCLATURE

A, concentration of species A, area;
B, concentration of species B;
D, molecular diffusivity;
d, diameter;
f, Fanning friction factor;
f', frequency [Hz];
k_c, mass-transfer coefficient defined by $N_A/A = k_c(A_w - A_{ave})$;
N_A, mass-transfer flux normal to the wall;
Re, Reynolds number (dU_{ave}/ν);
Sc, Schmidt number (ν/D);
Sh, Sherwood number, equation (9) ($k_c d/D$);
t, time;
U, vector instantaneous velocity;
U_{ave}, average velocity;
U_y^+, nondimensional y-velocity, equation (7);
U_x, U_y, U_z, velocity components;
u'_y, RMS value of $\bar{U}_y$;
u_x, u_y, u_z, fluctuating velocity components;
U^*, friction velocity;
X, normally distributed random variable;
x_A, mole fraction of species A;
x, y, z, space coordinates;
y, distance from the wall;
y^+, nondimensional distance, equation (7).

Greek symbols

ε, turbulent eddy diffusivity;
ε_y, eddy diffusivity for the scalar quantity;
ε_m, momentum diffusivity;
θ, duration of events;
ρ, density;
δ, order of magnitude;
μ, molecular viscosity;
ν, μ/ρ, the kinematic viscosity;
ϕ, dimensionless concentration, equation (7);
τ_w, wall shear stress;
ψ, dimensionless time, equation (7);
∇, del or nabla;
Δ, delta or difference.

Subscripts and superscripts

ave, average;
A, species A;
B, species B;
b, bulk;
max, maximum;
rc, random call;
w, wall;
–, overbar, time average;
′, RMS value.

INTRODUCTION

THERE are very many processes that in some way involve heat or mass transfer. One need only look at environmental, atmospheric, oceanographic, biomedical and chemical processing problems to find many examples. One of the most important operations in the chemical industry is mass or heat transfer at an interface. This occurs in nearly every unit operation; yet, in spite of its widespread practical application, it is poorly understood when the transfer between phases involves one phase in turbulent motion. This is due not so much to our deficient knowledge of the mass or heat transfer *per se*, but rather to our ignorance of the turbulence and our inability to characterize it in simple mathematical terms.

We know that when mass or heat transfer occurs from a tube to a fluid flowing turbulently within it, the

*K. N. McKelvey is now associated with The duPont Co., Wilmington, Del, U.S.A.

concentration or temperature gradient extends only a short distance from the wall for large Schmidt or Prandtl numbers. To study these processes we need only know the character of the turbulence in the wall area and understand its mechanisms. This will then enable modeling of the scalar field to be accomplished using a realistic picture of the turbulent flow field. The multitude of previous models have been based on long-time averages which do not adequately describe the turbulence characteristics.

Recent advances in understanding shear flow turbulence as a result of studies of coherent structures in the flow indicate a need for an approach that uses the unaveraged transport equations themselves. It is well known that the time averaging of the equation results in more unknowns than equations, which necessitates closure approximations, whereas the unaveraged equations can be solved, if the instantaneous velocity field is defined. Our purpose is to develop a physically realistic, mathematically solvable model of mass or heat transfer for this latter case. We want a model based directly on a knowledge of the statistics of wall turbulence and the molecular diffusivity of the material and not based on a mechanistic picture or on empirical parameters from mass-transfer data. An important added advantage of using the unaveraged equations approach is that information is obtained not just about the average characteristics but also about the fluctuating components of the scalar field. This latter is essential, if other than first order chemical kinetics are to be considered.

In order to simplify the further discussion, this paper will be written using mass-transfer terminology. It is a simple matter to convert the expressions to heat-transfer terminology. For the sake of consistency and ease of comparison, all expressions will be solved explicitly for the Sherwood number, which is a reduced mass transfer coefficient.

TURBULENCE NEAR THE WALL

The turbulent transfer of mass from a tube wall depends on both the molecular diffusion and the turbulent convective transport. The old notion that turbulent flow within tubes consists of three regions: (1) a turbulent central core in which viscous forces are unimportant, (2) a laminar sublayer near the wall in which eddy forces are insignificant and (3) a buffer zone between these two regions in which both viscous and eddy forces are important, has given way to a more modern concept of turbulence. This has been reviewed and discussed recently by Corino and Brodkey [1] and Nychas, Hershey and Brodkey [2]. The work of others has been extensively discussed in these references.

According to current ideas, the region $y^+ < 5$ is not a true laminar layer but is, instead, a viscous layer which is continually disturbed by small-scale fluctuations of low magnitude and intermittently disturbed by the intrusion of elements of fluid from $y^+ > 5$. In general, the motions in this layer are caused and sustained by motions in the adjacent region. The region $5 < y^+ < 70$, which approximately coincides with the buffer zone of the old concept, is by no means a "relatively passive transitional zone", but is instead a region of much activity. The most important feature of this area is the very intense, relatively small scale, three-dimensional ejections of fluid elements away from the wall ($5 < y^+ < 15$). These elements interact with a high shear zone ($7 < y^+ < 30$) causing intense, chaotic velocity fluctuations which at times cause disturbances that reach right to the wall.

For defining the turbulence field for use in the proposed calculation procedure, one needs to have detailed measurements of those structures that have been visually observed. For this we have used the results obtained by Wallace, Eckelmann and Brodkey [3], Brodkey, Wallace and Eckelmann [4] and Eckelmann [5]. In these works, the many contributions by others are reviewed and discussed and need not be repeated here.

MASS-TRANSFER MODELS

Mass-transfer models may be broken down into four general categories: (1) those based on the film theory, (2) those based on analogies between mass and momentum transfer (strictly speaking, these are analogies rather than models), (3) those which empirically allow some convective (eddy) transport near the wall and (4) those based on renewal theories. There have been many discussions of these in the literature. Rather than repeat such a review here, we will cite many of the references that also contain a review of the field. The most recent references that have a more direct bearing on the present work will be discussed.

As examples of those associated with allowing some eddy motion in the wall region, one can cite Murphree [6], Lin, Moulton and Putnam [7], Deissler [8], Notter and Sleicher [9], Higbie [10], Dankwerts [11], Hanratty [12], Toor and Marchello [13], Perlmutter [14], Harriott [15], Ruckenstein [16], Koppel, Patel and Holmes [17], Thomas and Fan [18, 19] and Bullin and Dukler [20]. Models have also been based on the concept of an unsteady boundary-layer type motion. Some of these are Einstein and Li [21], Ruckenstein [22], Black [23, 24], Meek and Baer [25, 26] and Pinczewski and Sideman [27].

Bullin and Dukler [28] have recently presented a stochastic model of turbulent diffusion. Their approach is based on the similarity of the mass transfer equation to the Fokker–Planck equation for a Markov process. They solved the corresponding Langevin equation by a hybrid computer technique, which is inherently faster than known methods using finite differences to solve the convective-diffusion equations. However, drastic assumptions must be made to relate the Lagrangian velocity in their formulation to Eulerian measures. Although Bullin and Dukler did not obtain RMS values, there is no basic reason why this could not have been done.

Besides the models of mass transfer which have been cited, there are numerous well-known empirical or semi-empirical equations. Two of the older, still widely used empirical equations are the Dittus–Boelter and

the Chilton–Colburn equations. More recent equations are those proposed by Metzner and Friend [29], Harriott and Hamilton [30] and Notter and Sleicher [9]. The best comparisons of the vast amount of data available can be found in [9] and [27].

PROPOSED MODEL

In contrast to all the references cited above the present work uses the unaveraged mass balance equation. For knowledge of the velocity field, a physical model is not used, but rather the velocity is matched, within a certain degree of approximation, to that actually observed in the experimental measurements cited [3–5].

The equation of mass continuity for any species A in a non-reacting system can be written as

$$(\partial A/\partial t)+(\mathbf{U}\cdot\nabla)A = D\nabla^2 A \tag{1}$$

where the concentration and velocity vector are instantaneous values, and the molecular diffusivity is assumed to be constant. For rectangular coordinates, this becomes

$$(\partial A/\partial t)+U_x(\partial A/\partial x)+U_y(\partial A/\partial y)+U_z(\partial A/\partial z) = D(\partial^2 A/\partial x^2+\partial^2 A/\partial y^2+\partial^2 A/\partial z^2). \tag{2}$$

If one is only concerned with a thin shell of thickness Δr, where $\Delta r \ll r$, the effect of curvature can be neglected and the equation can also be applied in the vicinity of the wall in pipe flow. The simplification of equation (2) used in this work is

$$(\partial A/\partial t)+U_y(\partial A/\partial y) = D(\partial^2 A/\partial y^2). \tag{3}$$

In order to arrive at equation (3), the following assumptions are necessary:

$$|\partial^2 A/\partial y^2| \gg |\partial^2 A/\partial x^2| \text{ and } |\partial^2 A/\partial z^2| \tag{4}$$

and

$$|U_y(\partial A/\partial y)| \gg |U_x(\partial A/\partial x)| \text{ and } |U_z(\partial A/\partial z)| \tag{5}$$

in the wall region. The justification for equation (4) is that, for high Schmidt number transfer, the dimension over which the concentration changes in the y-direction is an order of magnitude less than in the z-direction and at least this amount less in the x-direction. The y^+ dimension is less than 5, the lateral dimension (z^+) is of the order of 100 and the x^+ dimension as high as 1000 (see Kline *et al.* [31]). Thus, the term in $\partial^2/\partial y^2$ is two orders greater in size than the one in $\partial^2/\partial z^2$ and possibly as high as four orders greater than the one in $\partial^2/\partial x^2$. The justification for equation (5) is as follows:

$$\begin{aligned} U_y(\delta)[\partial A(1)/\partial y(\delta)] &= U_y(\partial A/\partial y)(1)\\ U_x(1)[\partial A(1)/\partial x(1/\delta^3)] &= U_x(\partial A/\partial x)(\delta^3)\\ U_z(\delta)[\partial A(1)/\partial z(1/\delta^2)] &= U_z(\partial A/\partial z)(\delta^3) \end{aligned} \tag{6}$$

where δ is the order of velocity and length and is an order less than unity. It is clear that the term in $\partial/\partial y$ is at least two orders of magnitude greater than that in $\partial/\partial x$ and $\partial/\partial z$ and may be as high as three orders greater. Sirkar and Hanratty [32] made a similar analysis and arrived at the same conclusions, independently. They considered two resulting equations, one for steady state and retaining the term in $\partial/\partial z$ and the other identical to equation (3).

Equation (3) can be transformed into the dimensionless form

$$\partial\phi/\partial\psi+(f/2)Re^2ScU_y^+(\partial\phi/\partial y^+) = (f/2)Re^2(\partial^2\phi/\partial y^{+2}) \tag{7}$$

where

$$\begin{aligned} \phi &= \phi(y,t) = (A-A_b)/(A_w-A_b)\\ y^+ &= yU^*/\nu\\ \psi &= Dt/d^2\\ U_y^+ &= U_y/U^*\\ U^* &= (\tau_w/\rho)^{1/2} = U_{x,\text{ave}}(f/2)^{1/2}. \end{aligned}$$

The molar flux of species A at the wall is given by

$$N_{A,w} = x_{A,w}(N_{A,w}+N_{B,w})-D(\partial A/\partial y)_w = -[D/(1-x_{A,w})](\partial A/\partial y)_w. \tag{8}$$

Equation (8) can be transformed into the dimensionless form

$$Sh = -(\partial\phi/\partial y^+)_{y^+=0}(f/2)Re. \tag{9}$$

Reasonable boundary conditions on $\phi(y,t)$ for equation (7) are

$$\begin{aligned} &\phi(y^+,0) = 0 \text{ or any other initializing condition}\\ &\phi(0,\psi) = 1\\ &\phi(L,\psi) = 0 \end{aligned} \tag{10}$$

where L, is chosen in this work to be 5. *Equations* (7) *and* (9) *along with the boundary conditions* (10) *and input data for* U_y^+ *comprise the model.*

The quantitative information about the radial velocity in the region $0 < y^+ < 5$ used in this work is based on the measurements reported by Wallace *et al.* [3], Brodkey *et al.* [4] and Eckelmann [5]. Details of the probability density distribution of U_y are given in [4]. The U_y distribution is much more symmetric than the U_x one and closer to Gaussian. Although not reported in [4], the skewness and flatness were measured. Over the range of $0 < y^+ < 10$, the average values were 0.53 and 4.3, respectively. For a Gaussian distribution these are 0 and 3. For this work, U_y was generated by the computer using a Gaussian random generator. The generated signal had zero mean, and RMS value as measured, and was truncated at the high and low ends to correspond to the reported distributions. These extremes were selected at the $y^+ = 5$ position and are $+4.01$ cm/s and -3.31 cm/s for the high and low ends. Other values were also tried, but there was no effect as such large extremes were rarely called.

Besides the distribution of magnitudes of the radial velocity, there is a length of time (or duration) over which the velocity fluctuation acts. A frequency, $1/\theta$, can be obtained from this duration. As a first approximation, it was assumed that at a given Reynolds

number the duration was constant. The information on this also came from [4], where the average duration (θ) of events is reported for the four classes of split signals. For this work, such a refined splitting was not attempted and an average duration at each available point ($y^+ = 3.4$, 6 and 10) was calculated by using the measured durations and the fraction of time the signal was in the various categories. The resulting time an eddy lasts was made non-dimensional with inner variables because only the area immediately adjacent to the wall was considered. The nondimensional duration varied little over the area and thus a single value was used for all y^+ positions. This value of $\theta U^{*2}/\nu$ was 8.0. The standard deviation about this at the three points was 0.46.

The final restriction necessary on the radial velocity is that its RMS value correspond to that actually measured over the region. For this, we fitted the measured wall region RMS data (Eckelmann [5]) with a fourth-order polynomial and required that the RMS values of the random data called fit the polynomial for each y^+ position. The fit used was

$$(\overline{U_y^{+2}})^{1/2} = Ay^+ + By^{+2} + Cy^{+3} + Dy^{+4} \quad (11)$$

and it was satisfactory out to a y^+ of 130, with $A = 5.10889 \times 10^{-2}$, $B = -9.23782 \times 10^{-4}$, $C = 7.00448 \times 10^{-6}$ and $D = -1.96310 \times 10^{-8}$. Equation (11) was used to generate the normal velocities from the random numbers by

$$U_y^+ = (\overline{U_y^{+2}})^{1/2} X \quad (12)$$

where X is normally distributed, random variable with respect to time, of variance equal to unity and mean equal to zero. As a consequence of the various assumptions, the fluid moves locally in a coherent manner. This is the type of behavior visually observed in this region [1].

In summary the following assumptions were made in this mathematical model: (1) The instantaneous concentration can be represented by equation (7), with the boundary conditions given by equation (10). (2) The instantaneous Sherwood number is given by equation (9). (3) The Schmidt number is high enough so that the instaneous normalized concentration at $y^+ = 5$ is essentially zero. (4) The instantaneous radial velocity in the sublayer is a result of motions in the adjacent layer, thus causing "connected motion" in the y-direction. With respect to time, the radial velocity is random and normally distributed with a mean of zero and a variance given by equation (11).

RESULTS AND DISCUSSION

In any numerical computation by finite difference, one must first establish that the numerical method itself does not influence the results. This involves the proper selection of both the space and time increments. For complete stability and convergence of the finite difference approximation, one should satisfy

$$\Delta y^+ \leqslant 2/(Sc U_y^+). \quad (13)$$

This condition is sufficient but not necessary for numerical accuracy; i.e. satisfactory results may well be obtained for Δy^+ values greater than given by equation (13), but this would have to be established by actual comparisons by numerical calculations. As a guide for Sc of 1000 and a reasonable maximum value of U_y^+ equation (13) gives $\Delta y^+ \leqslant 0.002$. For the maximum y^+ of 5 used in this work, this means 2500 space steps should give stability and convergence. However, the maximum Schmidt number of 6000 used would require six times the number of steps. The maximum value allowed for U_y^+ is at the most 4.01 times that obtained from equation (12) as given by the limits put on the distribution as previously mentioned. Equation (12) at y^+ of 5 gives $U_y^+ = 0.25$. We selected as a reasonable maximum $U_y^+ = 1$; i.e. four times the average, even though very rarely values as large as four times could occur. To check this numerically, runs were made with a fixed set of random numbers (so that the runs would be reproducible in detail) at a $Sc = 1000$ at space increments of 5000, 1000, 500, 250 and 125. For this, the time increment was selected such that eight numerical steps in time were made between each new selection of a random number to fix a new level of the normal velocity. When compared to the results obtained with 5000 space increments, those using 125 and 250 were unsatisfactory. At 500 increments, the results deviated more than is desirable at the outer boundary ($y^+ = 5$) and over the rest of the field were 1–2% high. The results using 1000 increments were similar to those from the 5000 increment run and about a 0.5% high. Since this is well within the expected accuracy of the model, 1000 space increments were used for further runs.

In order to check the size of the time step, runs were made with 16, 8, 4 and 2 time steps between each random call. When compared to the 16 time step run, the 2 time step run was unsatisfactory. The 4 time step run was low by about 3% for the average mass-transfer rate at the wall, high by about 6% for the concentration distribution. The 8 time step run reduced these errors by about half. Since, as will be seen, the model is only partially successful for predicting the concentration distribution, 4 or 5 time steps per random call were used for the final runs.

A critical estimate that had to be made was how long a run must be in order to have a preselected degree of reproducibility of the final averaged values when totally independent sequences of random numbers are used. For this we estimated the run times from the expression (14) obtained from Bendat and Piersol [33]:

$$\text{Percent reproducibility in final result} = 100(2t_{rc}/t_{\max})^{1/2} \quad (14)$$

where t_{rc} is the actual time between random calls and $t_{\max}$ is the total real run time. For all runs the value of $t_{\max}$ was selected so that the reproducibility as calculated from equation (14) was about 1%. To test this, runs under the same conditions but with totally different random sequences were made. The condition

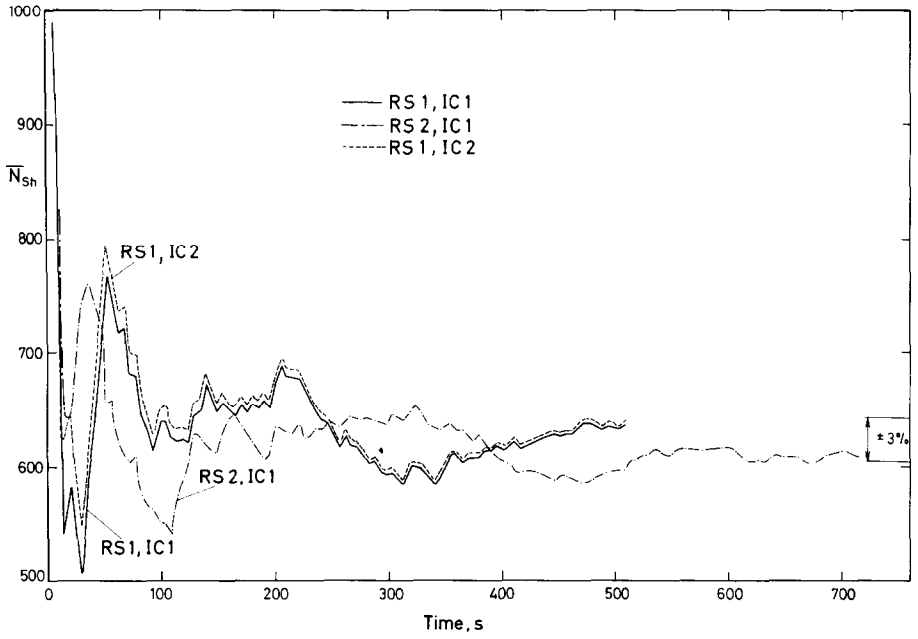

FIG. 1. Average Sherwood number at specific times. $Re = 10\,000$ and $Sc = 1000$. RS = random sequence and IC = initial condition.

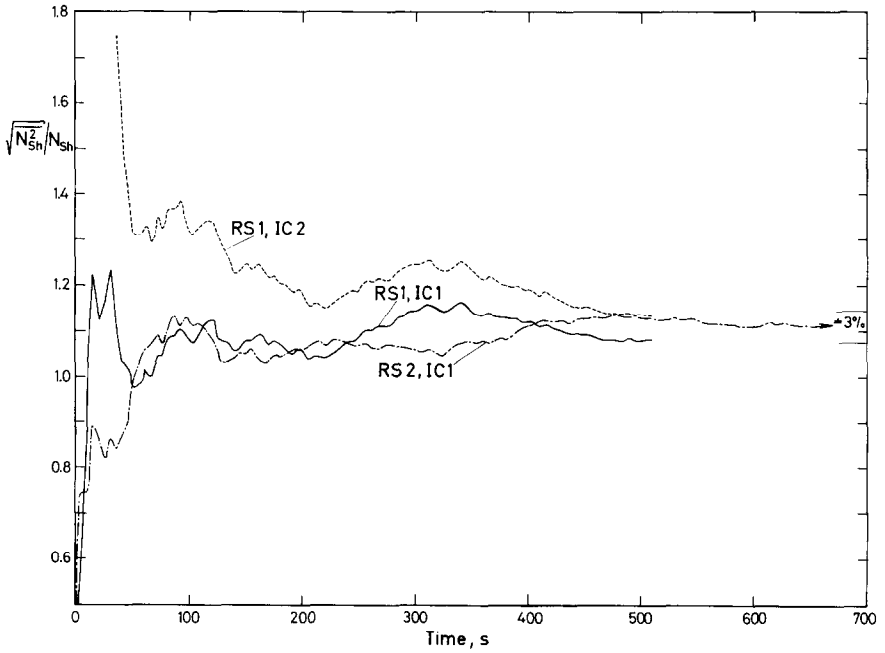

FIG. 2. RMS Sherwood number to average Sherwood number ratio. $Re = 10\,000$ and $Sc = 1000$. RS = random sequence and IC = initial condition.

selected was $Re = 10\,000$ and $Sc = 1000$. Figure 1 gives the results for the accumulative averaged Sherwood number ($\overline{Sh}$) and Fig. 2 for the ratio $Sh'/\overline{Sh}$. These two plots have expanded ordinates in order to emphasize the errors. Later plots on less expanded scales give a better feel for the approach to steady state. Also shown on these figures are runs with identical random sequences but with widely different initial conditions. For the average Sherwood number, the two runs with different random sequences were within $\pm 3\%$ of each other. Again, the estimate made from equation (14) for the three runs shown was between 1 and 15%. The RMS Sherwood number indicates similar behavior. Apparently the estimate by equation (14) is too low by about a factor of two. Although there is a wide discrepancy in the average Sherwood numbers for short times, after about 500 s of real time, the difference is negligible. The main initial condition (IC1) used to start the calculation was not far removed from the steady state concentration distribution calculated. The other (IC2) was purposely selected to deviate in the opposite direction and be far removed

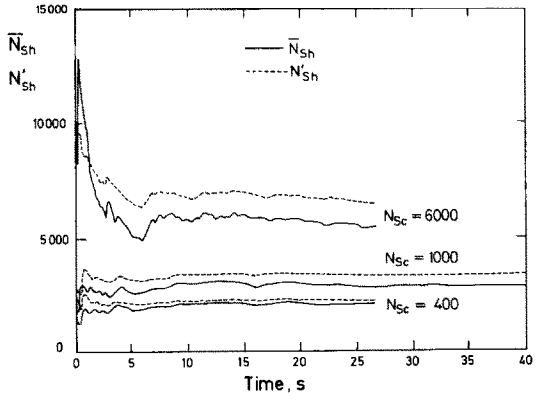

FIG. 3. Average Sherwood number at $Re = 60\,000$ for various Schmidt numbers.

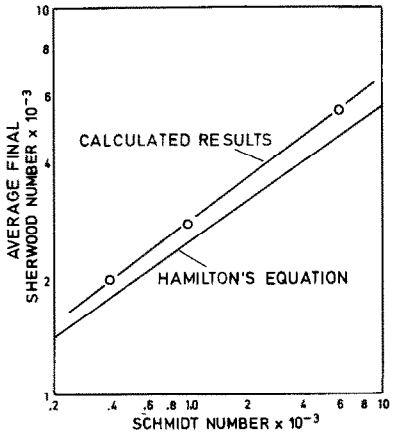

FIG. 4. Final average Sherwood number vs Schmidt number at $Re = 60\,000$.

from the steady state value. It was selected to be closer to a step input so as to make the runs with two different initial conditions as sensitive to the final conditions as possible. As seen in Fig. 1, the effect on the average Sherwood number is quite small, where the difference disappears after a short period of real time. For the RMS Sherwood number the effect was greater because of the initial high RMS values associated with the gradient being much different than the steady state value. It took a longer period of time to reduce the difference, but it was reduced to about $\pm 3\%$ after 500 s of real time.

Figure 3 shows the average and RMS Sherwood numbers as a function of time for three different Schmidt numbers at constant Reynolds number. The real times are such that the results should be within $\pm 3\%$ of the final values. This figure illustrates the correct increase of the Sherwood number with increasing Schmidt number. Figure 4 shows the average predicted Sherwood numbers at the ends of the runs vs Schmidt number compared to the equation of Hamilton [30]. The predicted variation of Sherwood number with Schmidt number is in good agreement with experimental values represented by Hamilton's equation, although possibly slightly high. Hamilton's equation is only an average representation of data that is widely scattered. Also recall that none of the parameters for the velocity field in the model were adjusted to fit the mass-transfer results.

The RMS values of the mass-transfer rate fluctuations are of the same order as the mean rate at the wall. This is a direct consequence of the RMS concentration gradient fluctuations at the wall being of the same order as the mean concentration gradient there (equation 9). Clearly, because of the small region over which the concentration changes, the turbulence can, for example, easily bring in fluid of zero concentration very close to the wall, thus resulting in high gradients. The only wall rate fluctuation data available is that of Sirkar and Hanratty [32] which, for $Sc \simeq 2300$, gave a RMS to mean ratio of 0.29. This is about one-quarter of our estimate. This must be a result of the limitations put on the instantaneous velocity in our model, such as the constant frequency for all events.

Figures 5 and 6 show the variation of the average Sherwood number with Reynolds number for Sc

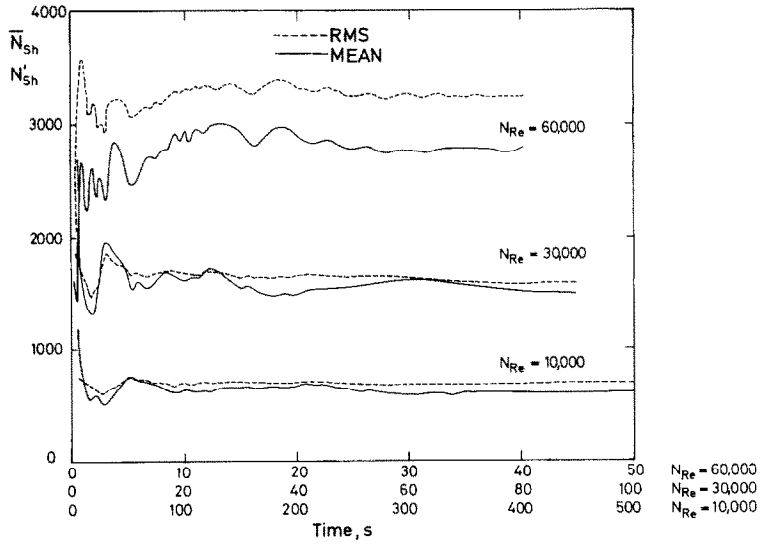

FIG. 5. Average Sherwood number at $Sc = 1000$ for various Reynolds numbers.

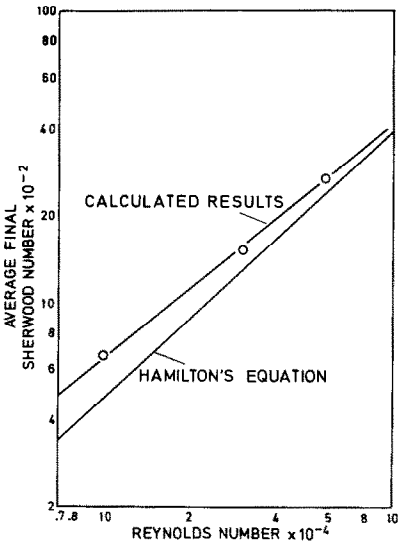

FIG. 6. Final average Sherwood number vs Reynolds number at $Sc = 1000$.

$= 1000$. Again, the agreement with Hamilton's equation is reasonable when one recognizes the scatter in the data that his equation represents.

Figure 7 shows the typical variation of the instantaneous Sherwood number with time. For the instantaneous values only every 500th time step was plotted, and, for this run, 500 steps represent 100 random calls. Clearly, if all steps were plotted, the signal would have much higher frequency content. The rate, which is plotted in Fig. 7, is very sensitive to changes in velocity. The concentration itself is less sensitive; thus, plots were generated that gave the location for a specific concentration for each time step. The plot was generated near the end of the run when steady state in the average values had been established.

Figures 8 and 9 show typical variations with time at steady state conditions of the position of fluid having an instantaneous normalized concentration less than 0.1 and the corresponding mass-transfer rate at the wall. The large ejections or excursions of high concentration fluid outward are the result of the particular

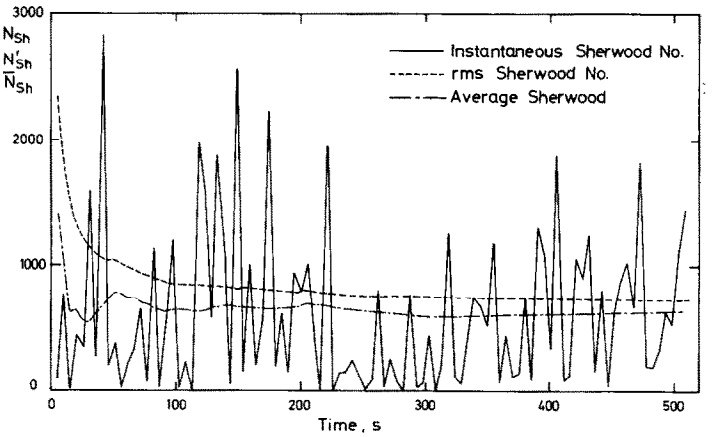

FIG. 7. Instantaneous RMS and average Sherwood numbers at $Re = 10\,000$ and $Sc = 1000$.

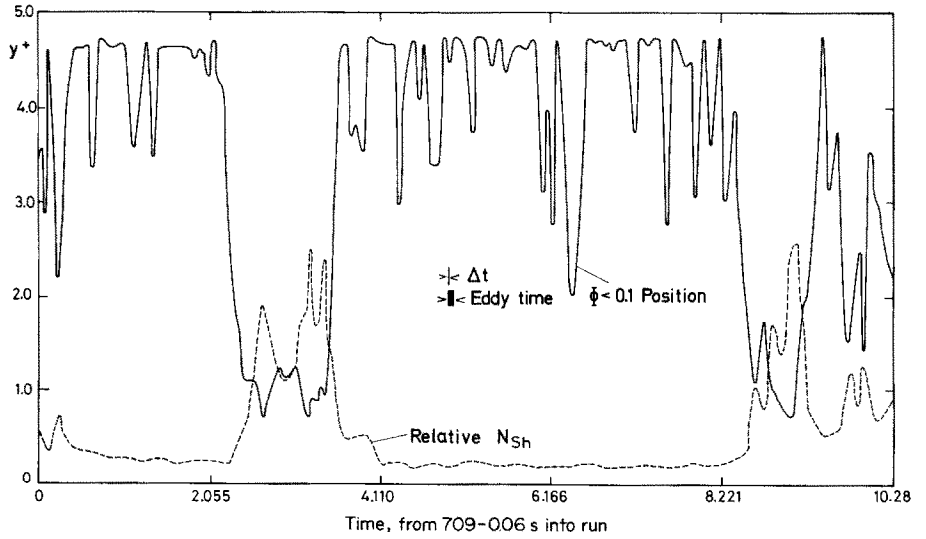

FIG. 8. Instantaneous position of fluid having $\phi = 0.1$ and instantaneous Sherwood number at $Re = 10\,000$ and $Sc = 1000$.

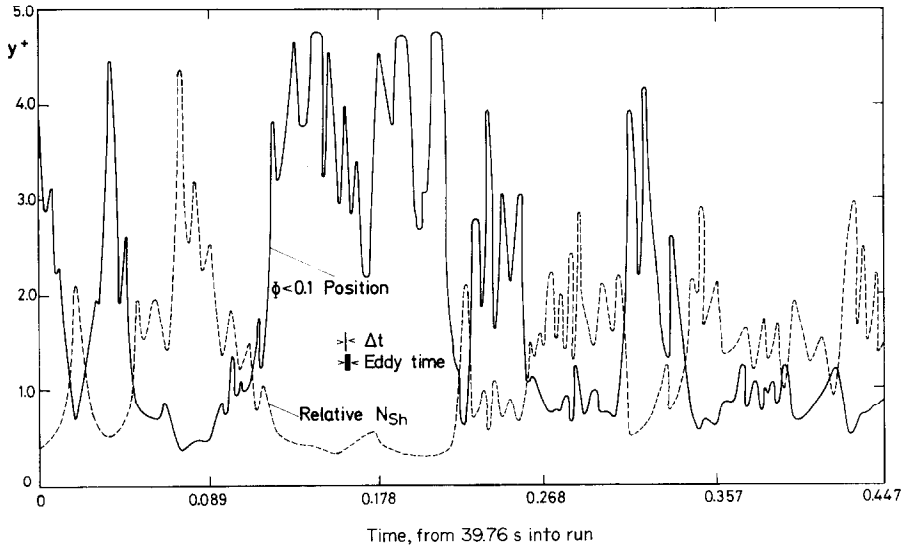

FIG. 9. Instantaneous position of fluid having $\phi = 0.1$ and instantaneous Sherwood number at $Re = 60\,000$ and $Sc = 1000$.

values of the random velocities generated. At first, it was difficult to understand how the instantaneous velocities could cause the concentration to vary so drastically, but when it is considered that $y^+ = 5$ corresponds, for these two Reynolds numbers, to distances of about 0.4 and less than 0.1 mm from the wall, respectively, the importance of small velocity in this area is better understood. The increase in the frequency with increasing Reynolds number is unmistakable, when one notes the time scale difference.

It is possible to compare the results of this model qualitatively with some of the experimental results obtained by Shaw and Hanratty [34] and Sirkar and Hanratty [32]. Since they used a probe of finite size, the variations in mass transfer are probably due only to rather large-scale variations in concentration. Shaw and Hanratty measured a frequency of mass-transfer coefficient fluctuations at $Re = 10\,000$ of about 0.3 Hz and at $Re = 60\,000$ of about 4 Hz. Sirkar and Hanratty presented the mass-transfer rate spectra for two Reynolds numbers. The peak region lies between 3.5 $\times 10^{-4} < f'v/U^{*2}$ 1.5×10^{-3}, which corresponds to 0.06–0.23 Hz for $Re = 10\,000$ and 1.3–5.4 Hz for 60 000. From Figs. 8 and 9 it can be calculated that the predicted frequencies of large-scale concentration fluctuations near the wall are in agreement with these measurements. Our values, which are very approximate are 0.2–0.3 Hz for a Reynolds number of 10 000

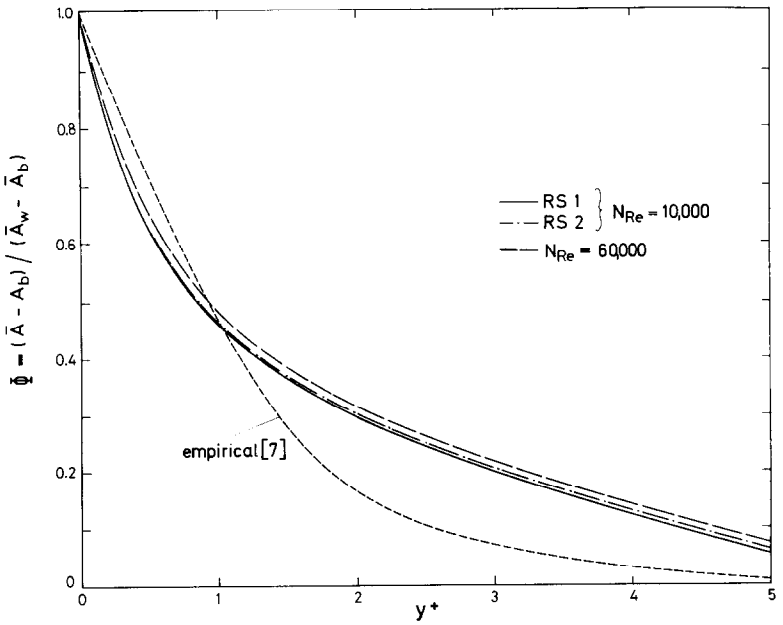

FIG. 10. Average concentration distribution at two Reynolds numbers and $Sc = 1000$. RS is random sequence selected.

and 6–11 Hz for 60 000. Note that the frequencies cited above are much lower than the basic frequency associated with velocity or the number of random calls/s. This is a result of the cascading effect of random numbers where often one will have a string of calls of the same sign and similar magnitude, so that the integral effect of one direction of transfer is retained for long periods of time.

Figure 10 shows a typical average concentration gradient along with that experimentally estimated from the results of Lin *et al.* [7]. The agreement with experiment is reasonably good for small values of y^+, but becomes progressively poorer as y^+ approaches 5. This result suggests that while the model adequately describes mass transfer in the immediate vicinity of the wall, it tends to break down as distance from the wall increases. This discrepancy is thought to be due to the assumption of a constant duration (i.e. random calls/s) of velocity fluctuations at a given Reynolds number. From Brodkey *et al.* [4] it is known that the durations of ejections (motions away from the wall) and sweeps (motions toward the wall) are not the same. Parenthetically, one may note that an ability to predict the mass-transfer coefficient is the least critical test of a model. Prediction of the concentration gradient is a more stringent test, a test most theories do not even attempt. The ultimate test would be the prediction of the concentration fluctuations which are also reported here and have not been reported elsewhere.

Some observations from the calculated results with regard to fluctuating quantities are of interest. The RMS Sherwood numbers have already been presented and discussed. The covariance, $\overline{u_y a}$, was in all cases linear in y^+ (up to y^+ of 5 used as the outer limit of the calculation). From this and the equation

$$\overline{u_y a} = \varepsilon_s(\mathrm{d}\bar{A}/\mathrm{d}y) \tag{15}$$

the scalar eddy viscosity was calculated and varied as y^{+2}, in contrast to the observed variation with y^{+3} [9]. However, the scalar eddy viscosity as calculated from equation (15) cannot really be relied upon because of the problems with the calculation of $\mathrm{d}\bar{A}/\mathrm{d}y$ as shown in Fig. 10. The linear variation of the covariance may also be a result of the fitting equation used in equation (11). Probably better would have been to use $A = 0$ and evaluate the other constants accordingly.

Over the range of variation in Reynolds number there was only a $\pm 3\%$ variation in the concentration profile and a $\pm 6\%$ variation in the scalar eddy viscosity. The inverse turbulent Prandtl number was less than unity over the y^+ range considered. Brodkey [36] suggested a parallel relation for the scalar field to that suggested for the momentum field by Brosko. The resulting approximation for the inverse turbulent Prandtl number is

$$\varepsilon_s/\varepsilon_m = (\mathrm{d}\bar{U}/\bar{U})/(\mathrm{d}\bar{A}/\bar{A}). \tag{16}$$

The inverse turbulent Prandtl number is indeterminate at the wall, but it approached zero in the numerical scheme as the wall was approached. From equation (16), the value approached infinity, indicating the approximation is not valid in the critical region near the wall.

Let us now consider the assumption of using constant duration or frequency of velocity fluctuations at a given Reynolds number in more detail. Passing through any point in the tube are eddies of various sizes. Most of these are probably near some average size, but a few will be much larger and a few much smaller. Since the velocity within an eddy is nearly constant, the velocity at the point being considered will be constant during the time it takes for the eddy to pass the point. Assuming that all of the eddies are convected at about the same velocity, then the frequency of velocity fluctuations will be very low when a large eddy is passing and high when a small eddy passes. Since the constant average frequency assumed in this model is probably representative of the average-sized eddies, the large and small ones are being neglected. Not considering the small eddies is probably of little consequence, but since the large eddies represent large movements of mass, they may contribute substantially to the mass transfer at the point even though they occur rather infrequently. This would lower the input of low concentration material from the outer region ($y^+ > 5$) and thus would predict less transfer between the region and the bulk stream than is experimentally observed. This is exactly what is shown in Fig. 10.

Since the mass transfer at the wall depends directly only on the conditions in the vicinity of the wall, it is possible to predict Sherwood numbers with reasonable accuracy with the assumption of a constant frequency of fluctuations. On the other hand, if the mass transfer throughout the region is to be adequately described, it will be necessary to assume a more realistic picture for the velocity fluctuations. The effort here was a first approximation to the actual observations, and as such was unique in that it is the first attempt to follow the instantaneous concentrations in the wall area using a realistic model. The fact that it is able to adequately predict Sherwood numbers is remarkable when it is considered that the model contains no adjustable constants. The value of the model, though, is not so much its ability to predict Sherwood number, but rather its ability to deal with the higher moments and to indicate the importance of various factors, such as the large eddies, on the mass transfer.

Acknowledgements—The authors wish to acknowledge the computer time given by the University and the Institute. The paper is in part based on the thesis work of McKelvey [37], completed in 1964 and presented at the Los Angeles Annual Meeting of the A.I.Ch.E. R. S. Brodkey received an Alexander von Humboldt Award for 1975, which made the final preparation of this paper possible.

REFERENCES

1. E. R. Corino and R. S. Brodkey, A visual study of the wall region in turbulent pipe flow, *J. Fluid Mech.* **37**, 1 (1969).
2. S. G. Nychas, H. C. Hershey and R. S. Brodkey, A visual study of turbulent shear flow, *J. Fluid Mech.* **61**, 513 (1973).

3. J. M. Wallace, H. Eckelmann and R. S. Brodkey, The wall region in turbulence signals in bounded shear flows, *J. Fluid Mech.* **54**, 39 (1972).
4. R. S. Brodkey, J. M. Wallace and H. Eckelmann, Some properties of truncated turbulence signals in bounded shear flows, *J. Fluid Mech.* **63**, 209 (1974).
5. H. Eckelmann, The structure of the viscous sublayer and the adjacent wall region in turbulent channel flow, *J. Fluid Mech.* **65**, 439 (1974).
6. E. V. Murphree, Relation between heat transfer and fluid friction, *Ind. Engng Chem.* **24**, 726 (1932).
7. C. S. Lin, R. W. Moulton and G. L. Putnam, Mass transfer between solid wall and fluid stream, *Ind. Engng Chem.* **45**, 636 (1953).
8. R. G. Deissler, Analysis of turbulent heat transfer, mass transfer, and friction in smooth tubes at high Prandtl or Schmidt numbers, NACA Report 1210 (1955).
9. R. H. Notter and C. A. Sleicher, The eddy diffusivity in the turbulent boundary layer near a wall, *Chem. Engng Sci.* **26**, 161 (1971).
10. R. Higbie, The rate of absorption of a pure gas into a still liquid during short periods of exposure, *Trans. Am. Instn Chem. Engrs* **31**, 365 (1935).
11. P. V. Dankwerts, Significance of liquid-film coefficients in gas absorption, *Ind. Engng Chem.* **43**, 1460 (1951).
12. T. J. Hanratty, Turbulent exchange of mass and momentum with a boundary, *A.I.Ch.E. Jl* **2**, 359 (1956).
13. H. L. Toor and J. M. Marchello, Film-penetration model for mass and heat transfer, *A.I.Ch.E. Jl* **4**, 97 (1958).
14. D. D. Perlmutter, Surface-renewal models in mass transfer, *Chem. Engng Sci.* **16**, 287 (1961).
15. P. Harriott, A random eddy modification of the penetration theory, *Chem. Engng Sci.* **17**, 149 (1962).
16. E. Ruckenstein, Some remarks on renewal models, *Chem. Engng Sci.* **18**, 233 (1963).
17. L. B. Koppel, R. D. Patel and J. T. Holmes, Statistical models for surface renewal in heat and mass transfer, *A.I.Ch.E. Jl* **12**, 941, 947 (1966).
18. L. C. Thomas and L. T. Fan, Adaptation of the surface rejuvenation model to turbulent heat and mass transfer at a solid–fluid interface, *I/EC Fundamentals* **10**, 135 (1971).
19. L. C. Thomas, Temperature profiles for turbulent flow in tubes and basic surface renewal models, *Chem. Engng Sci.* **26**, 1271 (1971).
20. J. A. Bullin and A. E. Dukler, Random eddy models for surface renewal: formulation as a stochastic process, *Chem. Engng Sci.* **27**, 439 (1972).
21. H. A. Einstein and H. Li, The viscous sublayer along a smooth boundary, *Trans. Am. Soc. Civ. Engrs* **82**, 293 (1956).
22. E. Ruckenstein, On solid–liquid mass transfer in turbulent pipe flow, *Chem. Engng Sci.* **22**, 474 (1967).
23. T. J. Black, A new model of the shear stress mechanism in wall turbulence, A.I.A.A. Preprint No. 68-42 (1968).
24. T. J. Black, Viscous drag reduction examined in the light of a new model of wall turbulence, in *Viscous Drag Reduction*, edited by C. S. Wells, p. 383. Plenum Press, New York (1969).
25. R. L. Meek and A. D. Baer, The periodic viscous sublayer in turbulent flow, *A.I.Ch.E. Jl* **16**, 841 (1970).
26. R. L. Meek and A. D. Baer, Turbulent heat transfer and the periodic viscous sublayer, *Int. J. Heat Mass Transfer* **16**, 1385 (1973).
27. W. V. Pinczewski and S. Sideman, A model for mass (heat) transfer in turbulent tube flow. Moderate and high Schmidt (Prandtl) numbers, *Chem. Engng Sci.* **29**, 1969 (1974).
28. J. A. Bullin and A. E. Dukler, Stochastic modeling of turbulent diffusion with hybrid computer, *Envir. Sci. Tech.* **8**, 156 (1974).
29. A. B. Metzner and W. L. Friend, Turbulent heat transfer inside tubes and the analogy among heat, mass and momentum transfer, *A.I.Ch.E. Jl* **4**, 393 (1958).
30. P. Harriott and R. M. Hamilton, Solid–liquid mass transfer in turbulent pipe flow, *Chem. Engng Sci.* **20**, 1073 (1965).
31. S. J. Kline, W. C. Reynolds, F. A. Schraub and P. W. Runstadler, The structure of turbulent boundary layers, *J. Fluid Mech.* **30**, 741 (1967).
32. K. K. Sirkar and T. J. Hanratty, Relation of turbulent mass transfer to a wall at high Schmidt numbers to the velocity field, *J. Fluid Mech.* **44**, 589 (1970).
33. J. S. Bendat and A. G. Piersol, *Random Data.* Wiley–Interscience, New York (1971).
34. P. V. Shaw and T. J. Hanratty, Fluctuations in the local rate of turbulent mass transfer to a pipe wall, *A.I.Ch.E. Jl* **10**, 475 (1964).
35. R. S. Brodkey, Limitations on a generalized velocity distribution, *A.I.Ch.E. Jl* **9**, 448 (1963).
36. R. S. Brodkey, Fluid motion and mixing, in *Mixing, Theory and Practice*, edited by V. Uhl and J. Gray, Vol. 1, Chapter 2. Academic Press, New York (1966).
37. K. N. McKelvey, Turbulent scalar transfer at high diffusivity ratios, M.S. Thesis in Chemical Engineering, The Ohio State University (1964).

TRANSFERT MASSIQUE ET PARIETAL RESULTANT DE STRUCTURES COHERENTES DANS UN LIQUIDE EN ECOULEMENT TURBULENT

Résumé—Un calcul numérique du transfert massique instantané sur une paroi solide est conduit à partir de l'équation de bilan massique monodimensionnel, l'information d'entrée étant la vitesse normale. Cette vitesse est générée sur l'ordinateur de façon à réaliser globalement la vitesse normale obtenue dans des expériences sur la turbulence. Le transfert massique moyen est prédit correctement. On considère d'autres caractéristiques du champ scalaire.

STOFFÜBERGANG AN DER WAND ALS ERGEBNIS KOHÄRENTER STRUKTUREN IN EINER TURBULENT STRÖMENDEN FLÜSSIGKEIT

Zusammenfassung– Mit Hilfe einer eindimensionalen Massenbilanz wurde der momentane Stoffübergang an einer festen Wand mit der Normalgeschwindigkeit als einziger Eingabegröße numerisch ermittelt. Diese Geschwindigkeit wurde vom Rechner selbst entsprechend der Charakteristik von Normalgeschwindigkeiten aus experimentellen Untersuchungen vorgegeben. Der mittlere Stoffübergang wurde in geeigneter Weise vorausberechnet. Andere Charakteristiken des skalaren Feldes werden mitgeteilt.

РАСЧЕТ МАССОПЕРЕНОСА У СТЕНКИ НА ОСНОВЕ ЭКСПЕРИМЕНТАЛЬНО УСТАНОВЛЕННОЙ СТРУКТУРЫ ТУРБУЛЕНТНОГО ПОТОКА ЖИДКОСТИ

Аннотация — Выполнен прямой численный расчет мгновенного массопереноса у твердой границы на основе одномерного уравнения баланса массы, когда известна только нормальная составляющая скорости на входе. На компьютере эта скорость генерируется таким образом, чтобы ее значения в основном соответствовали эксперименту. Средняя скорость массопереноса рассчитана с достаточной точностью. Приводятся также другие характеристики скалярного поля.